Recognition of 1,N^2-ethenoguanine by alkyladenine DNA glycosylase is restricted by a conserved active-site residue

Received for publication, October 11, 2019, and in revised form, December 19, 2019 Published, Papers in Press, December 27, 2019, DOI 10.1074/jbc.RA119.011459

Adam Z. Thelen and Patrick J. O'Brien[1]

From the Department of Biological Chemistry, University of Michigan, Ann Arbor, Michigan 48109-0600

Edited by Patrick Sung

The adenine, cytosine, and guanine bases of DNA are susceptible to alkylation by the aldehyde products of lipid peroxidation and by the metabolic byproducts of vinyl chloride pollutants. The resulting adducts spontaneously cyclize to form harmful etheno lesions. Cells employ a variety of DNA repair pathways to protect themselves from these pro-mutagenic modifications. Human alkyladenine DNA glycosylase (AAG) is thought to initiate base excision repair of both 1,N^6-ethenoadenine (ϵA) and 1,N^2-ethenoguanine (ϵG). However, it is not clear how AAG might accommodate ϵG in an active site that is complementary to ϵA. This prompted a thorough investigation of AAG-catalyzed excision of ϵG from several relevant contexts. Using single-turnover and multiple-turnover kinetic analyses, we found that ϵG in its natural ϵG·C context is very poorly recognized relative to ϵA·T. Bulged and mispaired ϵG contexts, which can form during DNA replication, were similarly poor substrates for AAG. Furthermore, AAG could not recognize an ϵG site in competition with excess undamaged DNA sites. Guided by previous structural studies, we hypothesized that Asn-169, a conserved residue in the AAG active-site pocket, contributes to discrimination against ϵG. Consistent with this model, the N169S variant of AAG was 7-fold more active for excision of ϵG compared with the wildtype (WT) enzyme. Taken together, these findings suggest that ϵG is not a primary substrate of AAG, and that current models for etheno lesion repair in humans should be revised. We propose that other repair and tolerance mechanisms operate in the case of ϵG lesions.

All cellular life contends with the challenge of DNA alkylation damage. DNA bases are alkylated by both endogenous and exogenous compounds, and the failure to repair these base lesions results in a variety of deleterious consequences ranging from point mutations to the stalling of DNA replication or transcription (1). Etheno lesions represent a subset of exocyclic alkylation adducts that can arise through alkylation of purine and pyrimidine bases of genomic DNA (Fig. 1) (2). The etheno lesions 1,N^6-ethenoadenine (ϵA),[2] N^2,3-ethenocytosine (ϵC), 1,N^2-ethenoguanine (ϵG), and N^2,3-ethenoguanine (N^2,3-ϵG) are naturally formed through exposure to the reactive aldehyde products of lipid peroxidation and subsequent ring closure (3, 4). Notably, etheno lesions have also been shown to arise due to reactions with chloroacetaldehyde and other metabolic byproducts of the common industrial compound vinyl chloride (5). *In vitro* DNA replication assays have demonstrated the miscoding properties of etheno lesions as well as the propensity for them to halt replication (6–8). Consistent with these deleterious effects on DNA replication, etheno lesions have cytotoxic effects on mammalian cells (9).

The base excision repair (BER) pathway exists in all domains of life, and it is responsible for removing and replacing diverse single nucleotide lesions such as those that arise through DNA alkylation, oxidation, and deamination (10). BER is initiated by a DNA glycosylase that searches DNA to locate specific sites of DNA damage and catalyzes the excision of the base lesion to generate an abasic site. Subsequent action by an AP endonuclease, dRP lyase, DNA polymerase, and DNA ligase nicks the backbone at the abasic site, removes the deoxy sugar, inserts an undamaged base to complement the opposing strand, and ligates the nick.

Alkyladenine DNA glycosylase (AAG) utilizes a nucleotide flipping mechanism to target a broad range of alkylated DNA lesions (11–13). Upon specific binding of the enzyme to a target lesion, the lesion is rotated out of the duplex and into the enzyme active site for cleavage. AAG was initially proposed to repair all of the etheno adducts that can arise in human cells (14). ϵA is a well-characterized substrate of human AAG, and it is recognized with high affinity by the enzyme *in vitro* (11, 15). AAG also recognizes and binds to sites of ϵC damage, however, it is unable to catalyze cleavage of the *N*-glycosidic bond (16). Rather, the human glycosylases TDG and SMUG1, along with the direct reversal protein AlkBH2, have been shown to repair ϵC (17–19).

Compared with ϵC and ϵA, less is known about the repair of ϵG. *In vitro* reactions between DNA and aldehydes derived from lipid peroxidation favor the production of ϵG over N^2,3-ϵG, indicating that ϵG might be the more relevant natural lesion (20–22). The opposite appears to be true of damage originating from exposure to vinyl chloride and its byproducts (20, 23). ϵG

This work was supported by a University of Michigan Department of Biological Chemistry graduate student award, Chemistry/Biology Interface Training Program fellowship from the NIGMS, National Institutes of Health Grants T32GM008597 (to A. Z. T.) and R01GM108022 (to P. J. O.), and National Science Foundation Grant MCB-1615586 (to P. J. O.). The authors declare that they have no conflicts of interest with the contents of this article. The content is solely the responsibility of the authors and does not necessarily represent the official views of the National Institutes of Health. This article contains Figs. S1–S4.

[1] To whom correspondence should be addressed. Tel.: 734-647-5821; Fax: 734-763-4581; E-mail: pjobrien@umich.edu.

[2] The abbreviations used are: ϵA, 1,N^6-ethenoadenine; ϵC, N^2,3-ethenocytosine; ϵG, 1,N^2-ethenoguanine; N^2,3-ϵG, N^2,3-ethenoguanine; AAG, alkyladenine DNA glycosylase (also known as MPG, methylpurine DNA glycosylase); BER, base excision repair.

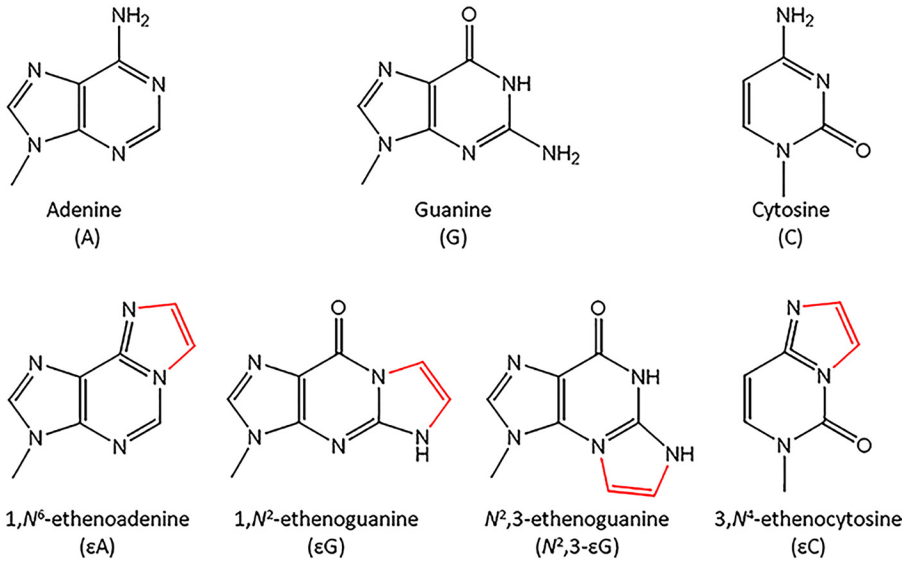

Figure 1. Diverse structures of the etheno DNA lesions. The four etheno lesions are depicted below their undamaged forms.

causes both replication blocks and a mixture of G → T and G → C transversion mutations in mammalian cells (6, 7). The lesion also blocks transcription by enzymes such as human RNA polymerase II (24). The exact frequency of ϵG lesions in the human genome is not firmly established, however, the harmful effects of unrepaired ϵG combined with the natural origin of the lesion suggest that there must be a means of repairing the lesion.

AAG was previously investigated for glycosylase activity toward ϵG (14, 25, 26). Although these studies conclude that AAG catalyzes the excision of ϵG, the kinetics of that excision vary widely between reports (25, 26). The relevance of the N-terminal domain of AAG for ϵG recognition is also contentious. The N-terminal 79 residues of human AAG form a flexible region that is not conserved among different species. One study concluded that truncation of the N terminus of human AAG eliminated activity toward ϵG (25), whereas a subsequent study reported similar activity of full-length and N terminally truncated AAG toward ϵG (26). However, this second study reported a very low percentage (6%) of ϵG could be excised. Studies employing different base lesion substrates concluded that the truncation of the N terminus reduces the searching efficiency of AAG, but does not significantly affect the rate constant for *N*-glycosidic bond cleavage *in vitro* (27, 28).

In this work we characterized the single- and multiple-turnover kinetics of the AAG-catalyzed excision of ϵG from a variety of DNA duplexes. Comparison of the kinetic constants for excision of ϵG and ϵA, and the results of direct competition experiments, together demonstrate that ϵG is a very poor substrate of AAG. We investigated the structural origins for this substrate specificity and found that mutation of Asn-169 to a smaller side chain allows significantly increased activity toward ϵG, presumably because the bulky etheno adduct can be better accommodated in the active site. Although we have verified the claims that AAG is capable of catalyzing excision of ϵG *in vitro*, our work argues against this being a *bona fide* physiological substrate and leads to the prediction that other DNA repair pathways are responsible for ϵG repair *in vivo*.

Results and discussion

Multiple-turnover kinetics of AAG-catalyzed excision of ϵG

To examine the kinetics of ϵG excision by human AAG, we expressed and purified Δ80 AAG from *Escherichia coli* for *in vitro* glycosylase assays. We used steady-state kinetics to characterize the efficiency of AAG-catalyzed excision of ϵG from a 25-mer DNA duplex containing a central ϵG·C target site (see "Experimental procedures"). Reaction conditions were selected to maximize the activity of AAG while maintaining enzyme stability over a long time course, and linear initial rates were observed up to 10% product formation with no evidence of a pre-steady-state burst (Fig. 2*A*). Despite the optimized conditions for AAG activity, the reaction proceeded slowly with a k_{cat} of 0.0048 min^{-1} (Fig. 2*B*). The catalytic efficiency of the reaction, given by k_{cat}/K_m, was measured to be 220 M^{-1} s^{-1}. In comparison, the catalytic efficiency of AAG for excision of ϵA, a well-characterized substrate, has been estimated to be 4 orders of magnitude higher under the same conditions (11). This discrepancy is conspicuous given the similar origin and the mutagenicity of both lesions.

To more directly compare the efficiencies for the excision of ϵG and ϵA, the lesion-containing oligonucleotides were competed in the same glycosylase assay mixture. The ϵG lesion was paired with a complementary C, whereas the ϵA lesion was paired with a complementary G. The ϵA·G pairing is the least efficient base pairing for ϵA excision, potentially allowing for the relatively slow ϵG excision to compete (29). To distinguish the ϵA and ϵG DNA substrates and products on a gel, the ϵG lesion was incorporated into a 25-mer DNA sequence, whereas the ϵA lesion was incorporated in a 19-mer DNA sequence. We controlled for the effect of DNA length on the kinetics of glycosylase activity by performing a competition assay between ϵA incorporated into the 19- and 25-mer sequences. No substantial preference between the 19- and 25-mer was observed (Fig. S1). The formation of the fluorescently labeled 12- and 9-mer products from excision of ϵG and ϵA, respectively, was monitored to obtain initial rates for the excision of both substrates.

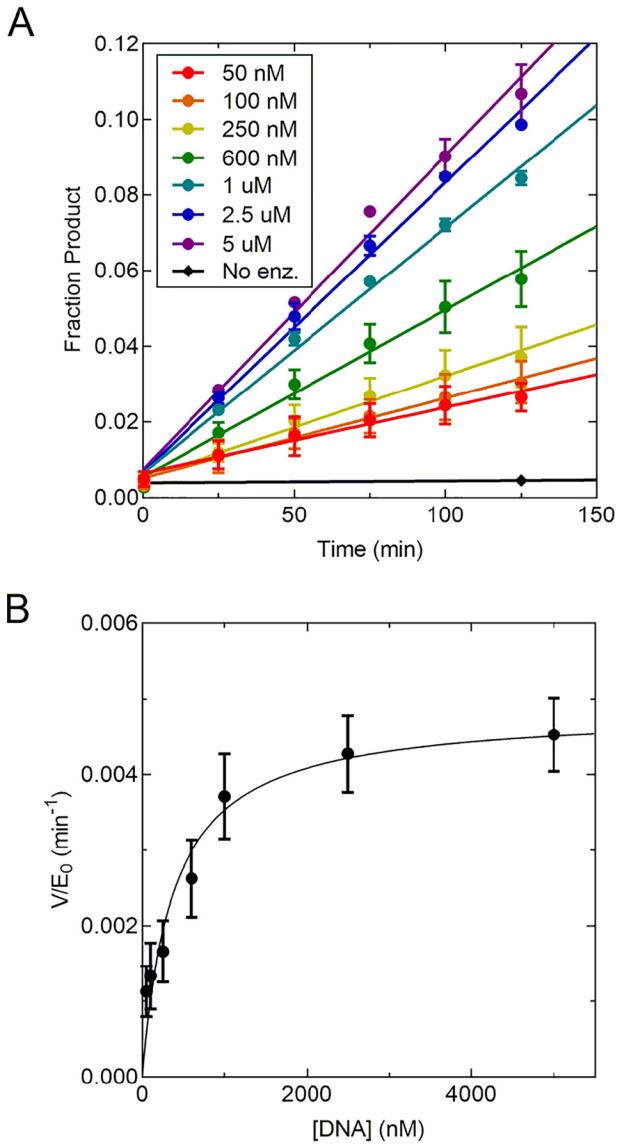

Figure 2. Multiple-turnover excision of ϵG by AAG. *A,* time course of the Δ80 AAG-catalyzed excision of ϵG from a 25-mer DNA substrate with an opposing C base. Concentrations of DNA are listed in the legend, with DNA in 50-fold excess of enzyme for each reaction. *Error bars* represent the S.D. of 2 trials. *B,* dependence of ϵG excision rate on DNA concentration, fit to a hyperbola with $k_{cat} = 0.0048$ min^{-1} and $K_m = 370$ nM. Points represent the average of 4 replicates, and *error bars* represent the S.D.

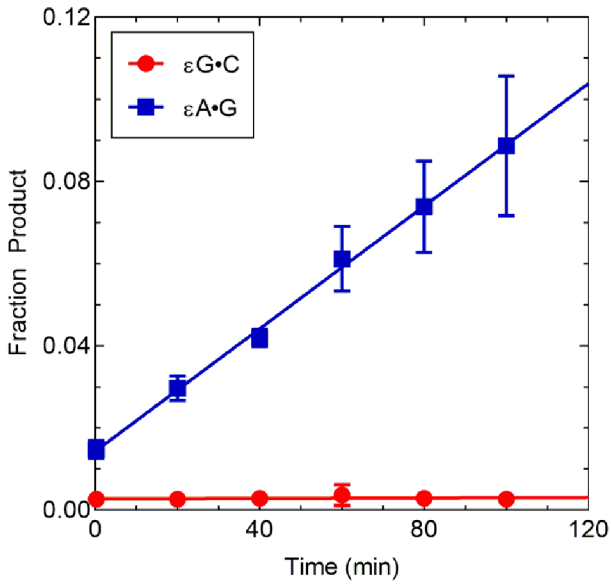

Figure 3. Competition of ϵG and ϵA for AAG-catalyzed excision. Reactions contained 2 nM Δ80 AAG, 2 μM ϵG in the 25-mer DNA sequence with an opposing C, and 200 nM ϵA in the 19-mer DNA sequence with an opposing G. *Lines* of best fit were calculated using linear regression. Points represent the average of 4 replicates, and *error bars* represent the S.D.

At a ratio of 10:1 ϵG to ϵA, no detectable ϵG product was formed during the initial period of the ϵA reaction (Fig. 3). As 0.5% of the ϵG excision product could have been reliably detected, we conservatively estimate that ϵA·G is preferred over ϵG·C by at least 200-fold. These data further support the conclusion that ϵG is poorly recognized relative to primary substrates of AAG.

AAG-catalyzed single-turnover excision of ϵG

Single-turnover glycosylase reactions were performed to measure the rate of ϵG and ϵA excision catalyzed by AAG. These reactions report on all the steps preceding and including *N*-glycosidic bond cleavage, but subsequent steps such as product release are excluded. To directly compare with previous results, an optimal pH of 6.1 was used (28), and AAG was up to 3-fold more active for excision of ϵG at pH 6.1 as compared with pH 7.5 (Fig. S2). Each single-turnover reaction of ϵG excision proceeded to ~85% completion, indicating the presence of a small quantity of nonreactive species in the ϵG-DNA (Fig. 4, *A* and *B*). As observed in the multiple-turnover experiments, AAG-catalyzed excision of ϵG proceeded more slowly than excision of ϵA. Furthermore, the concentration dependence of Δ80 AAG exhibited biphasic behavior (Fig. 4*C*, *red squares*).

In the classic model for single-turnover kinetics, the relationship between k_{obs} and the concentration of enzyme should fit to a hyperbola. However, a reduction in the rate constant for excision of ϵG was observed at elevated concentrations of AAG (Fig. 4*C*). A similar inhibitory effect was previously reported for the *E. coli* 3-methyladenine DNA glycosylase (AlkA), but this is the first instance of such behavior from AAG (30). Using the inhibition model developed for AlkA, described in Fig. S4, a K_i value of 680 nM was determined for Δ80 AAG. These concentrations of AAG far exceed cellular conditions, making such enzyme crowding unlikely in a cellular context. However, the inability of AAG to distinguish ϵG from undamaged sites could have serious physiological implications.

To assess the relative affinity of AAG for undamaged and damaged sites, single-turnover reactions of AAG with ϵG and ϵA were challenged with varying concentrations of undamaged 25-mer DNA oligonucleotides containing a central A·T pair. The excision of ϵA was unaffected by the presence of undamaged DNA, up to at least 80-fold excess over the damaged DNA, which was the highest concentration tested (Fig. 5). In contrast, the excision of ϵG was strongly inhibited by the presence of undamaged DNA, with an IC_{50} of 400 nM. This experiment indicates that ϵG·C is preferred by a factor of 300-fold relative to binding to undamaged sites, which is much less than the lower limit of >30,000 preference for ϵA·T. The 300-fold preference for ϵG·C, relative to a typical

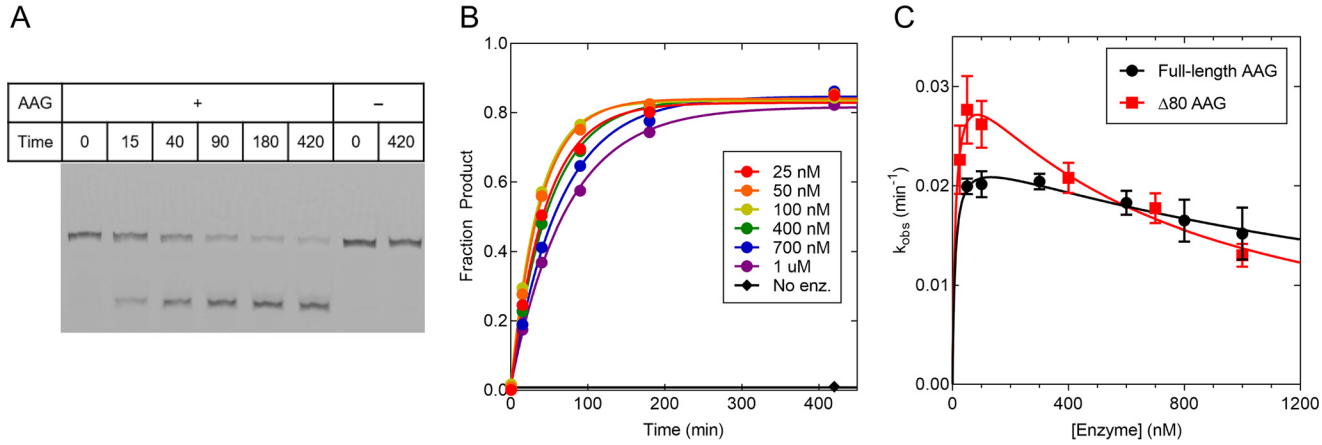

Figure 4. Single-turnover excision of ϵG by AAG. *A,* representative gel for the AAG-catalyzed single-turnover excision of ϵG. Reactions contained 20 nM 25-mer DNA with ϵG complemented by a *C*. Enzyme concentration was varied between reactions. Pictured are reactions with or without 400 nM Δ80 AAG. *B,* time courses for ϵG excision by Δ80 AAG. Enzyme concentrations are indicated in the legend. *C,* the single-turnover rate constants for ϵG excision catalyzed by both full-length and Δ80 AAG are shown plotted by enzyme concentration. Reactions contained 20 nM ϵG in the 25-mer DNA sequence. The values were fit to the multivalent interference model detailed in Fig. S4. Points for full-length AAG represent the mean of 4 replicates, whereas points for 80 AAG represent the mean of 6 replicates. *Error bars* represent the S.D. For Δ80 AAG the best fit values are $k_{max} = 0.034$ min^{-1}, $K_{1/2} = 11$ nM, and $K_i = 680$ nM. For full-length AAG the values are $k_{max} = 0.024$ min^{-1}, $K_{1/2} = 9$ nM, and $K_i = 2.0$ μM.

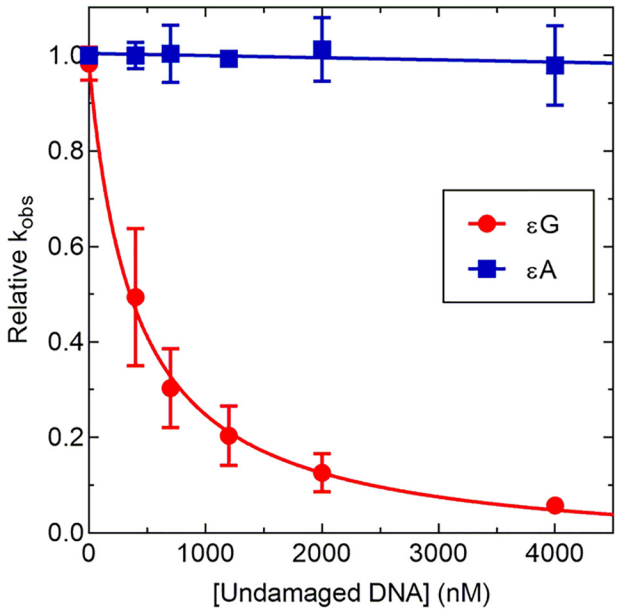

Figure 5. Competition of AAG-catalyzed excision of ϵG and ϵA by undamaged DNA. Reactions containing 100 nM Δ80 AAG and 50 nM of lesion-containing substrate were incubated with increasing concentrations of undamaged 25-mer DNA. The loss of ϵG excision activity was fit with Equation 5, producing an IC_{50} of 400 nM. Points represent the mean of 4 replicates, and *error bars* represent the S.D.

undamaged DNA site, is unlikely to be sufficient for repair in the cell where there is a vast excess of undamaged relative to damaged sites.

The N-terminal region of AAG is not necessary for the excision of ϵG

Previous studies have demonstrated that the catalytic domain of AAG is more stable than the full-length protein and has similar rates of *N*-glycosidic bond cleavage with many different substrates (27, 28). Despite this, it has been reported that ϵG in particular cannot be excised by N-terminal truncations of AAG (25). Our multiple-turnover and single-turnover glycosylase assays indicate the contrary, that Δ80 AAG is active toward ϵG under a variety of conditions. However, differences may still exist between the two protein variants. To compare the activity of full-length and truncated AAG, we repeated the single-turnover glycosylase assays with full-length AAG (Fig. 4*C*, *black circles*). Both full-length and Δ80 AAG were able to reach similar end points with comparable k_{max} values. Similar to the truncated protein, the $K_{1/2}$ for ϵG excision by full-length AAG was too low to accurately measure. The full-length protein also displayed inhibition at high enzyme concentrations, although to a lesser degree than the truncated protein. These results support the model that the N-terminal region of AAG is unnecessary for catalytic activity.

AAG recognizes ϵG poorly in other relevant DNA contexts

The oligonucleotides used in the preceding assays represent the expected context for the alkylation of a G·C pair to form an ϵG lesion. However, other pairings can occur during replication of the damaged template (6, 7). We characterized the single-turnover kinetics of ϵG·T excision and found rates similar to those of ϵG·C excision (Table 1). AAG exhibited similar enzyme concentration-dependent inhibition for excision of ϵG from ϵG·T as was observed for ϵG·C (Fig. S3). The similar glycosylase activity with either opposing pyrimidine is consistent with the similar multiple-turnover rates of excision that were previously reported (25). These results demonstrate that the inhibition of ϵG excision by excess AAG molecules is not exclusive to a single base complement.

During replication of ϵG, DNA polymerases can slip to generate a −1 frameshift (31, 32). The slippage event places the ϵG lesion into a bulged context without a complementary base. Previously it was shown that AAG excises ϵA and Hx from a bulged context at comparable rates to base-paired contexts (33, 34). To assess the ability of AAG to recognize ϵG from a bulged conformation, single-turnover glycosylase assays were performed with a 25-mer bulged substrate (Fig. 6). Notably, the bulged lesion appeared to lack the concentration-dependent inhibitory effect observed with ϵG base pairs and the data could

Table 1
Maximum rate constants for the AAG-catalyzed single-turnover excision of ϵG

Values are reported for Δ80 AAG at 37 °C in a buffer containing 50 mM NaMES (pH 6.1), 10% glycerol, 0.1 mg/ml of BSA, 1 mM DTT, 1 mM EDTA, and 100 mM ionic strength adjusted with NaCl. Each value represents the average of ≥3 replicates. Reactions were fit to the biphasic model detailed in Fig. S4 and the maximum single turnover rate constant k_{max} for the first phase in each reaction are listed.

Lesion	k_{max}
	min^{-1}
ϵG·C	0.034 ± 0.005
ϵG·T	0.032[a]
ϵG bulge	0.0057 ± 0.0003
ϵA·T	0.23 ± 0.015

[a] The maximum rate constant was calculated from the average of 2 replicates (Fig. S3).

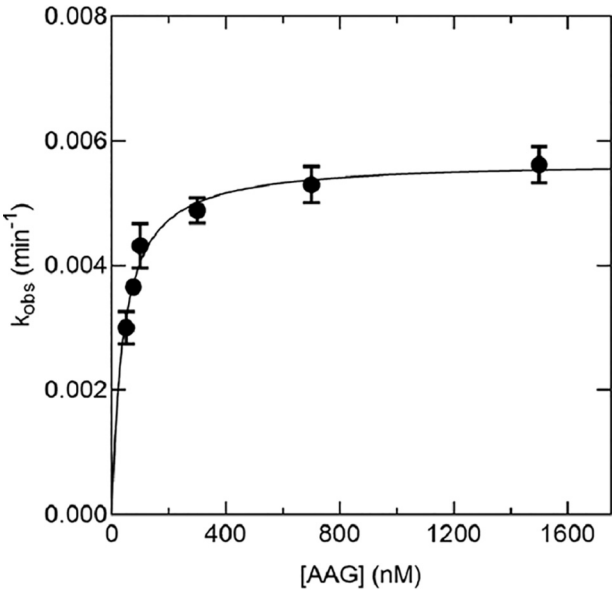

Figure 6. Single-turnover excision of ϵG from a bulged substrate. The observed single-turnover rate constants for the excision of bulged ϵG were plotted against varying concentrations of Δ80 AAG. A k_{max} value of 0.0057 min^{-1} was determined, with a $K_{1/2}$ value of 40 nM. Reactions contained 20 nM 25-mer bulge DNA with the ϵG lesion. Points represent the mean of 4 replicates, and *error bars* indicate the S.D.

be readily fit to a typical hyperbolic concentration dependence. It is not clear why there was not an inhibitory effect at high concentrations of AAG, but it is possible that the presence of the bulge structure disrupts the competing nonspecific DNA-binding sites that allows for better equilibration between the specific lesion site and the competing nonspecific sites. However, the bulged ϵG substrate was excised with a 10-fold lower k_{max} value than was observed for the duplex ϵG·C substrate (Table 1). This observation suggests that ϵG is inefficiently recognized in the bulged context, whereas AAG readily recognizes other base lesions in the same bulged context (33, 34). An NMR structure of the ϵG bulge DNA (35) shows that the unpaired ϵG can be accommodated within the DNA duplex. It appears that this stable structure limits the ability of AAG to gain access and flip out the lesion, as compared with ϵG mispairs. Although AAG is capable of excising ϵG from a bulged context *in vitro*, it is clear that this is not a favorable context for AAG-initiated repair of ϵG.

Asn-169 of AAG limits the rate of ϵG excision

Crystal structures of AAG bound to a flipped-out ϵA lesion revealed how this active site pocket can accommodate base lesions and exclude undamaged bases (13). The side chain of Asn-169 defines one surface of the active site, closely contacting the N1 face of the ϵA lesion (Fig. 7*A*). This residue plays a role in blocking the binding of undamaged guanine with its N^2-amino group (11, 36), leading us to consider whether this side chain might also make contact with the 1,N^2-etheno ring of ϵG. We used site-directed mutagenesis to generate variants of Δ80 AAG with either a serine or an alanine residue in place of Asn-169, and subsequently determined the impact of these mutations on the single-turnover excision kinetics of ϵA and ϵG.

The N169A mutation caused an increase in the k_{max} value for ϵG excision from 0.034 to 0.041 min^{-1} and the inhibition at high concentrations of enzyme was much less prominent as compared with the behavior of the WT enzyme (Fig. 7*B*; Table 2). This increase in the excision rate of the N169A mutant suggests that Asn-169 interferes with the excision of ϵG to some degree. Surprisingly, the k_{max} for ϵA excision was also substantially increased by the N169A mutation (Fig. 7*C*). This likely reflects a removal of a deleterious interaction between the Asn-169 side chain and the ϵA lesion or could result from rearrangements in the Ala variant that create more favorable interactions with the substrate.

The N169S mutation is a more conservative change to the active site structure, as it maintains hydrogen bonding capability while shortening the side chain length to expand the binding pocket. The N169S variant displayed a dramatic elevation in the k_{max} values for excision of both ϵG and ϵA (Fig. 7*C*). However, the N169S mutant enhanced ϵG excision by more than 7-fold, whereas only increasing ϵA excision by 2-fold (Fig. 7*D*). The greater activity of N169S relative to N169A suggests the possibility of positive hydrogen bonding interactions for the serine side chain that were lacking in the alanine substitution. The N169S mutant also showed little to no enzyme concentration-dependent inhibition of ϵG excision, even up to concentrations several times higher than those tested for the WT enzyme. This absence of detectable inhibition can be explained by the previously proposed inhibition model, whereby the stronger recognition of ϵG by the N169S variant would enable the lesion to compete more favorably with undamaged sites for binding and excision. The observation that ϵG excision by AAG is improved by mutation of Asn-169 is consistent with the model that this side chain clashes with the ϵG lesion and contributes to its inefficient excision by AAG.

Conclusions

The exocyclic ring structure of the mutagenic and cytotoxic lesion ϵG presents a unique challenge for recognition by the DNA base excision repair pathway. It has previously been postulated that base excision repair initiated by AAG is the preferred mechanism for repair of both ϵA and ϵG (14, 25, 26). Herein, we demonstrated that ϵG is excised with much lower efficiency than other primary substrates of AAG under both single- and multiple-turnover conditions. We also provide the

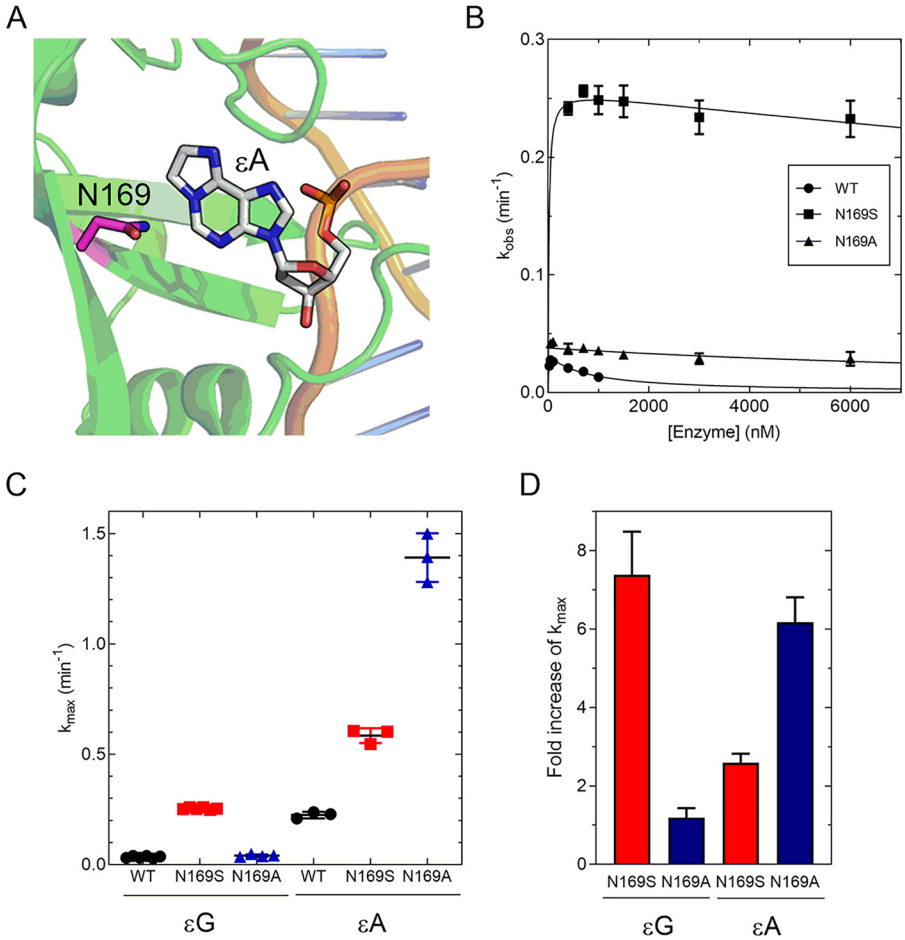

Figure 7. Asn-169 of AAG restricts excision of ϵG. *A,* in crystal structures of AAG bound to ϵA, the side chain of Asn-169 is in close proximity to N^1 and C^2 of the nucleobase. If ϵG were to bind in the same conformation its exocyclic ring is predicted to clash with the side chain of Asn-169. *B,* single-turnover rate constants for the excision of ϵG, catalyzed by variants of Δ80 AAG. Reactions contained 20 nM ϵG in the 25-mer DNA sequence with a C complement. Rate constants for WT are replotted from Fig. 4*C*, whereas data for N169S and N169A represent the average of 4 replicates. *Error bars* represent the S.D. *C,* the maximum single-turnover rate constants from *panel B* are plotted alongside values for ϵA excision. *D,* the fold-increase in the maximum single-turnover rate constant due to each AAG mutation. Each value is calculated by dividing the values of k_{max} for the variant enzyme by the k_{max} for the WT enzyme. *Error bars* represent the propagated error of both measured values.

Table 2

Maximum rate constants for the single-turnover excision of ϵG and ϵA by WT and mutant AAG

Values are reported for Δ80 AAG at 37 °C in a buffer containing 50 mM NaMES (pH 6.1), 10% glycerol, 0.1 mg/ml BSA, 1 mM DTT, 1 mM EDTA, and 100 mM ionic strength adjusted with NaCl. Each value represents the average of ≥3 replicates.

AAG Variant	k_{max}	
	ϵG·C[a]	ϵA·T[b]
	min^{-1}	
WT	0.034 ± 0.005	0.23 ± 0.015
N169S	0.25 ± 0.004	0.58 ± 0.034
N169A	0.041 ± 0.006	1.4 ± 0.11

[a] Reactions with ϵG·C were fit to the biphasic model detailed in Fig. S4 and the maximum single-turnover rate constant k_{max} for the first phase in each reaction are listed.
[b] Reactions with ϵA·T were determined from exponential fits at saturating enzyme concentration of 1 μM.

first examination of competition between undamaged and ϵG-containing DNA, demonstrating that AAG has a difficult time recognizing ϵG sites.

Our findings highlight some of the limitations of single-turnover kinetic approaches to studying DNA repair glycosylases with defined homogenous substrates. Whereas experiments with simple substrates are indispensable for quantitative analysis and the dissection of individual reaction steps, these assays neglect the impact of relevant cellular factors such as excess undamaged DNA and bound histone proteins. We infer that inhibition of ϵG excision at higher concentration of AAG protein is indicative of relatively poor lesion recognition, such that nonspecific binding modes compete with the lesion-specific binding mode, and this has now been observed for both AAG and *E. coli* AlkA (30). We demonstrated that nonspecific competitor DNA competes effectively for binding of AAG to the ϵG lesion, suggesting that it would be difficult for AAG to effectively locate these lesions in the nucleus. The packaging of DNA into nucleosome core particles presents another potential challenge for the repair of ϵG in cells, as nucleosomes have been shown to restrict AAG and other glycosylases from accessing sites of DNA damage (37, 38).

To provide a physical explanation for the discrimination by AAG against ϵG, we have shown that residue Asn-169 limits the ability of AAG to excise ϵG from DNA. This is consistent with the model that Asn-169 plays a crucial role in governing the selectivity of the enzyme against substrates with a functional group at the C2 position (13, 36). Mutation of Asn-169 results

```
25mer          5′ – (FAM) CGATAGCATCCTXCCTTCTCTCCAT
               3′ –       GCTATCGTAGGAYGGAAGAGAGGTA

19mer          5′ –       (FAM) TAGCATCCTXCCTTCTCTC
               3′ –             ATCGTAGGAYGGAAGAGAG

25mer bulge    5′ – (FAM) CGATAGCATCCTXCCTTCTCTCCAT
               3′ –       GCTATCGTAGGA-GGAAGAGAGGTA

X: εG, εA, Hx  Y: C, T
```

Scheme 1.

in a substantial increase in the excision of undamaged G from mispairs, a promutagenic change that could offset the benefit of a more versatile active site (36, 39, 40). The inability of AAG to efficiently catalyze the excision of ϵG may reflect a tradeoff for greater specificity and discrimination against undamaged G nucleotides that are present in great excess within the genome (11, 36).

In light of the dangers posed to the cell by unrepaired ϵG lesions, the inability of AAG to efficiently excise ϵG suggests that other repair pathways are likely to bear primary responsibility for protecting the genome against this particular lesion. Previous *in vitro* studies of the human homologs of AlkB, which catalyze oxidative dealkylation of certain alkylated bases, demonstrates that ALKBH2, but not ALKBH3, is capable of recognizing and repairing ϵG in duplex context (41). Although ALKBH2 is a strong candidate for physiological repair of ϵG·C, it is not known if this enzyme is able to capture rare ϵG lesions from among the excess of undamaged sites and it is not known how ϵG might be recognized in post-replicative repair. Although ϵG has not been specifically investigated, genetic studies of mice lacking AAG, ALKBH2, or ALKBH3 show increased sensitivity to induced colitis (42). Strong synergy was observed when all three genes were knocked out, demonstrating redundancy in the repair of DNA alkylation damage *in vivo* (42). More research is needed to decipher the complexities of substrate specificity in mammalian alkylation repair.

Experimental procedures

Preparation of DNA

Undamaged oligonucleotides were synthesized by Integrated DNA Technologies, and lesion-containing oligonucleotides were synthesized by the W. M. Keck Facility at Yale University(Scheme 1). The lesion-containing strand of each oligonucleotide was labeled at the 5′ end with 6-fluorescein (FAM). Oligonucleotides were purified via denaturing PAGE, and the concentrations were determined by the theoretical extinction coefficient at 260 nm as described previously (27).

Preparation of enzymes

The catalytic domain of AAG (Δ80 AAG) was expressed and purified from *E. coli* C41(DE3) as described previously (28). The construct for N169S was previously described (11) and the N169A mutation was generated by site-directed mutagenesis and confirmed by sequencing both strands of the ORF. These two variant AAG proteins were expressed and purified using the same methods. Full-length AAG was expressed and purified as described previously (43). The concentration of each AAG variant was initially estimated using UV absorbance and the active concentration of each enzyme was established through analysis of the burst kinetics for excision of hypoxanthine (Hx) as described previously (27).

Multiple-turnover glycosylase assay

Reactions were performed at 37 °C in reaction buffer containing 50 mM NaHEPES (pH 7.5), 10% glycerol, 0.1 mg/ml of BSA, 1 mM DTT, 1 mM EDTA, and 100 mM ionic strength adjusted with NaCl. The DNA concentration was kept at a 50:1 ratio relative to the AAG concentration to ensure multiple-turnover conditions. Aliquots were removed from the reactions at various time points and were quenched in an equal volume of 0.4 M NaOH to reach 0.2 M NaOH final concentration. The quenched aliquots were heated at 70 °C for 12 min to cleave abasic sites, and then were mixed 1:2 with loading buffer (90% formamide, 10 mM EDTA, 0.025% bromphenol blue, 0.025% xylene cyanol). For time courses lasting longer than 24 h, quenched samples were stored at 4 °C for no more than 12 h before being heated and mixed with loading buffer. The samples were run out on 20% polyacrylamide gels containing 6.6 M urea and scanned with an Amersham Biosciences Typhoon 5 Biomolecular Imager (GE Healthcare Life Sciences). The samples were excited at 488 nm and the emission of fluorescein was measured with a 525BP20 filter. The bands on the gel were quantified using ImageQuant TL (GE Healthcare). The fraction product (product/(substrate + product)) was calculated for each lane, and the steady-state formation of product was fit with linear regression. The change in observed reaction velocity at varying DNA concentrations was fit to the Michaelis-Menten equation (Equation 1).

$$V_{obs} = \frac{k_{cat}[E][S]}{K_M + [S]} \quad \text{(Eq. 1)}$$

V_{obs} represents the observed initial reaction velocity, k_{cat} the steady-state rate constant, [E] the concentration of enzyme, [S] the concentration of substrate, and K_m the Michaelis constant, equal to the concentration of DNA at the half-maximal velocity.

Single-turnover glycosylase assay

To achieve single-turnover conditions, glycosylase assays were performed with 10–20 nM DNA and 50 nM to 6 μM enzyme in reaction buffer containing 50 mM NaMES (pH 6.1), 10% glycerol, 0.1 mg/ml of BSA, 1 mM DTT, 1 mM EDTA, and 100 mM ionic strength adjusted with NaCl. All reactions were performed at 37 °C. Aliquots were quenched and quantified as described above. Reactions were fit to a single exponential according to Equation 2.

$$\text{Fraction product} = A(1 - e^{-k_{obs}t}) + c \quad \text{(Eq. 2)}$$

A represents the amplitude, k_{obs} the observed single-turnover rate constant, t the reaction time, and c the starting amount of abasic DNA. The dependence of the single-turnover rate constant, k_{obs}, on enzyme concentration was fit by a hyperbola according to Equation 3 in which k_{max} represents the maximum k_{obs} value and $K_{½}$ represents the concentration at which enzyme is half-saturating.

$$k_{obs} = \frac{k_{max}[E]}{K_{1/2} + [E]} \quad \text{(Eq. 3)}$$

For reactions demonstrating enzyme-dependent inhibition, a multivalent inhibitory model was applied, in which K_i is the binding constant for the inhibitory complex (Equation 4).

$$k_{obs} = \frac{k_{max}[E]}{K_{1/2} + [E]\left(1 + \frac{[E]}{K_i}\right)} \quad \text{(Eq. 4)}$$

This model has been used previously for the nonspecific binding of another DNA glycosylase to multiple DNA sites (30). For the titration of undamaged DNA, the IC_{50} was calculated using Equation 5, where k_{obs} is the observed rate constant, k_{unin} is the rate constant without undamaged DNA inhibitor, and I is the concentration of undamaged inhibitor DNA.

$$k_{obs} = \frac{k_{unin}[I]}{IC_{50} + [I]} \quad \text{(Eq. 5)}$$

Author contributions—A. Z. T. and P. J. O. conceptualization; A. Z. T. investigation; A. Z. T. writing-original draft; P. J. O. funding acquisition; P. J. O. project administration; P. J. O. writing-review and editing.

Acknowledgments—We thank Erin Taylor for preliminary observations and purified oligonucleotides, Michael Baldwin for purified full-length AAG, Karina Kangas for purified Δ80 AAG, and members of the O'Brien lab for helpful discussion.

References

1. Lindahl, T. (1993) Instability and decay of the primary structure of DNA. *Nature* **362,** 709–715 CrossRef Medline
2. Beranek, D. T. (1990) Distribution of methyl and ethyl adducts following alkylation with monofunctional alkylating agents. *Mutat. Res.* **231,** 11–30 CrossRef Medline
3. Gros, L., Ishchenko, A. A., and Saparbaev, M. (2003) Enzymology of repair of etheno-adducts. *Mutat. Res.* **531,** 219–229 CrossRef Medline
4. Kochetkov, N. K., Shibaev, V. N., and Kost, A. A. (1971) New reaction of adenine and cytosine derivatives, potentially useful for nucleic acids modification. *Tetrahedron Lett.* **12,** 1993–1996 CrossRef
5. Guengerich, F. P. (1992) Roles of the vinyl chloride oxidation products 1-chlorooxirane and 2-chloroacetaldehyde in the *in vitro* formation of etheno adducts of nucleic acid bases [corrected]. *Chem. Res. Toxicol.* **5,** 2–5 CrossRef Medline
6. Langouët, S., Müller, M., and Guengerich, F. P. (1997) Misincorporation of dNTPs opposite 1,*N*2-ethenoguanine and 5,6,7,9-tetrahydro-7-hydroxy-9-oxoimidazo[1,2-a]purine in oligonucleotides by Escherichia coli polymerases I exo- and II exo-, T7 polymerase exo-, human immunodeficiency virus-1 reverse transcriptase, and rat polymerase *β*. *Biochemistry* **36,** 6069–6079 CrossRef Medline
7. Choi, J. Y., Zang, H., Angel, K. C., Kozekov, I. D., Goodenough, A. K., Rizzo, C. J., and Guengerich, F. P. (2006) Translesion synthesis across 1,N2-ethenoguanine by human DNA polymerases. *Chem. Res. Toxicol.* **19,** 879–886 CrossRef Medline
8. Langouët, S., Mican, A. N., Müller, M., Fink, S. P., Marnett, L. J., Muhle, S. A., and Guengerich, F. P. (1998) Misincorporation of nucleotides opposite five-membered exocyclic ring guanine derivatives by *Escherichia coli* polymerases in vitro and in vivo: 1,N2-ethenoguanine, 5,6,7,9-tetrahydro-9-oxoimidazo[1,2-a]purine, and 5,6,7,9-tetrahydro-7-hydroxy-9-oxoimidazo[1, 2-a]purine. *Biochemistry* **37,** 5184–5193 CrossRef Medline
9. Akasaka, S., and Guengerich, F. P. (1999) Mutagenicity of site-specifically located 1,N2-ethenoguanine in Chinese hamster ovary cell chromosomal DNA. *Chem. Res. Toxicol.* **12,** 501–507 CrossRef Medline
10. Krokan, H. E., and Bjorås, M. (2013) Base excision repair. *Cold Spring Harb. Perspect. Biol.* **5,** a012583 Medline
11. O'Brien, P. J., and Ellenberger, T. (2004) Dissecting the broad substrate specificity of human 3-methyladenine-DNA glycosylase. *J. Biol. Chem.* **279,** 9750–9757 CrossRef Medline
12. Wolfe, A. E., and O'Brien, P. J. (2009) Kinetic mechanism for the flipping and excision of 1,N^6-ethenoadenine by human alkyladenine DNA glycosylase. *Biochemistry* **48,** 11357–11369 CrossRef Medline
13. Lau, A. Y., Wyatt, M. D., Glassner, B. J., Samson, L. D., and Ellenberger, T. (2000) Molecular basis for discriminating between normal and damaged bases by the human alkyladenine glycosylase, AAG. *Proc. Natl. Acad. Sci. U.S.A.* **97,** 13573–13578 CrossRef Medline
14. Dosanjh, M. K., Chenna, A., Kim, E., Fraenkel-Conrat, H., Samson, L., and Singer, B. (1994) All four known cyclic adducts formed in DNA by the vinyl chloride metabolite chloroacetaldehyde are released by a human DNA glycosylase. *Proc. Natl. Acad. Sci. U.S.A.* **91,** 1024–1028 CrossRef Medline
15. Rydberg, B., Dosanjh, M. K., and Singer, B. (1991) Human cells contain protein specifically binding to a single 1,N6-ethenoadenine in a DNA fragment. *Proc. Natl. Acad. Sci. U.S.A.* **88,** 6839–6842 CrossRef Medline
16. Lingaraju, G. M., Davis, C. A., Setser, J. W., Samson, L. D., and Drennan, C. L. (2011) Structural basis for the inhibition of human alkyladenine DNA glycosylase (AAG) by 3,N^4-ethenocytosine-containing DNA. *J. Biol. Chem.* **286,** 13205–13213 CrossRef Medline
17. Fu, D., and Samson, L. D. (2012) Direct repair of 3,N(4)-ethenocytosine by the human ALKBH2 dioxygenase is blocked by the AAG/MPG glycosylase. *DNA Repair* **11,** 46–52 CrossRef Medline
18. Kavli, B., Sundheim, O., Akbari, M., Otterlei, M., Nilsen, H., Skorpen, F., Aas, P. A., Hagen, L., Krokan, H. E., and Slupphaug, G. (2002) hUNG2 is the major repair enzyme for removal of uracil from U:A matches, U:G mismatches, and U in single-stranded DNA, with hSMUG1 as a broad specificity backup. *J. Biol. Chem.* **277,** 39926–39936 CrossRef Medline
19. Goto, M., Shinmura, K., Matsushima, Y., Ishino, K., Yamada, H., Totsuka, Y., Matsuda, T., Nakagama, H., and Sugimura, H. (2014) Human DNA glycosylase enzyme TDG repairs thymine mispaired with exocyclic etheno-DNA adducts. *Free Radic. Biol. Med.* **76,** 136–146 CrossRef Medline
20. Morinello, E. J., Ham, A. J., Ranasinghe, A., Sangaiah, R., and Swenberg, J. A. (2001) Simultaneous quantitation of N(2),3-ethenoguanine and 1,N^2-ethenoguanine with an immunoaffinity/gas chromatography/high-resolution mass spectrometry assay. *Chem. Res. Toxicol.* **14,** 327–334 CrossRef Medline
21. Sattsangi, P. D., Leonard, N. J., and Frihart, C. R. (1977) 1,N2-Ethenoguanine and N2,3-ethenoguanine: synthesis and comparison of the electronic spectral properties of these linear and angular triheterocycles related to the Y bases. *J. Org. Chem.* **42,** 3292–3296 CrossRef Medline
22. Sodum, R. S., and Chung, F. L. (1988) 1,N2-ethenodeoxyguanosine as a potential marker for DNA adduct formation by trans-4-hydroxy-2-nonenal. *Cancer Res.* **48,** 320–323 Medline
23. Müller, M., Belas, F. J., Blair, I. A., and Guengerich, F. P. (1997) Analysis of 1,N2-ethenoguanine and 5,6,7,9-tetrahydro-7-hydroxy-9-oxoimidazo[1,2-a]purine in DNA treated with 2-chlorooxirane by high performance liquid chromatography/electrospray mass spectrometry and comparison of amounts to other DNA adducts. *Chem. Res. Toxicol.* **10,** 242–247 CrossRef Medline
24. Dimitri, A., Goodenough, A. K., Guengerich, F. P., Broyde, S., and Scicchitano, D. A. (2008) Transcription processing at 1,N2-ethenoguanine by human RNA polymerase II and bacteriophage T7 RNA polymerase. *J. Mol. Biol.* **375,** 353–366 CrossRef Medline
25. Saparbaev, M., Langouët, S., Privezentzev, C. V., Guengerich, F. P., Cai, H., Elder, R. H., and Laval, J. (2002) 1,N^2-ethenoguanine, a mutagenic DNA adduct, is a primary substrate of *Escherichia coli* mismatch-specific uracil-DNA glycosylase and human alkylpurine-DNA-*N*-glycosylase. *J. Biol. Chem.* **277,** 26987–26993 CrossRef Medline

26. Lee, C. Y., Delaney, J. C., Kartalou, M., Lingaraju, G. M., Maor-Shoshani, A., Essigmann, J. M., and Samson, L. D. (2009) Recognition and processing of a new repertoire of DNA substrates by human 3-methyladenine DNA glycosylase (AAG). *Biochemistry* **48,** 1850–1861 CrossRef Medline
27. Hedglin, M., and O'Brien, P. J. (2008) Human alkyladenine DNA glycosylase employs a processive search for DNA damage. *Biochemistry* **47,** 11434–11445 CrossRef Medline
28. O'Brien, P. J., and Ellenberger, T. (2003) Human alkyladenine DNA glycosylase uses acid-base catalysis for selective excision of damaged purines. *Biochemistry* **42,** 12418–12429 CrossRef Medline
29. Biswas, T., Clos, L. J., 2nd, SantaLucia, J., Jr., Mitra, S., and Roy, R. (2002) Binding of specific DNA base-pair mismatches by *N*-methylpurine-DNA glycosylase and its implication in initial damage recognition. *J. Mol. Biol.* **320,** 503–513 CrossRef Medline
30. Zhao, B., and O'Brien, P. J. (2011) Kinetic mechanism for the excision of hypoxanthine by *Escherichia coli* AlkA and evidence for binding to DNA ends. *Biochemistry* **50,** 4350–4359 CrossRef Medline
31. Chang, S. C., Fedeles, B. I., Wu, J., Delaney, J. C., Li, D., Zhao, L., Christov, P. P., Yau, E., Singh, V., Jost, M., Drennan, C. L., Marnett, L. J., Rizzo, C. J., Levine, S. S., Guengerich, F. P., and Essigmann, J. M. (2015) Next-generation sequencing reveals the biological significance of the N^2,3-ethenoguanine lesion *in vivo*. *Nucleic Acids Res.* **43,** 5489–5500 CrossRef Medline
32. Zang, H., Goodenough, A. K., Choi, J. Y., Irimia, A., Loukachevitch, L. V., Kozekov, I. D., Angel, K. C., Rizzo, C. J., Egli, M., and Guengerich, F. P. (2005) DNA adduct bypass polymerization by *Sulfolobus solfataricus* DNA polymerase Dpo4: analysis and crystal structures of multiple base pair substitution and frameshift products with the adduct 1,N^2-ethenoguanine. *J. Biol. Chem.* **280,** 29750–29764 CrossRef Medline
33. Lyons, D. M., and O'Brien, P. J. (2009) Efficient recognition of an unpaired lesion by a DNA repair glycosylase. *J. Am. Chem. Soc.* **131,** 17742–17743 CrossRef Medline
34. Lyons, D. M., and O'Brien, P. J. (2010) Human base excision repair creates a bias toward −1 frameshift mutations. *J. Biol. Chem.* **285,** 25203–25212 CrossRef Medline
35. Shanmugam, G., Kozekov, I. D., Guengerich, F. P., Rizzo, C. J., and Stone, M. P. (2010) Structure of the 1,N^2-etheno-2′-deoxyguanosine lesion in the 3′-G(ϵdG)T-5′ sequence opposite a one-base deletion. *Biochemistry* **49,** 2615–2626 CrossRef Medline
36. Connor, E. E., and Wyatt, M. D. (2002) Active-site clashes prevent the human 3-methyladenine DNA glycosylase from improperly removing bases. *Chem. Biol.* **9,** 1033–1041 CrossRef Medline
37. Kennedy, E. E., Caffrey, P. J., and Delaney, S. (2018) Initiating base excision repair in chromatin. *DNA Repair* **71,** 87–92 CrossRef Medline
38. Kennedy, E. E., Li, C., and Delaney, S. (2019) Global repair profile of human alkyladenine DNA glycosylase on nucleosomes reveals DNA packaging effects. *ACS Chem. Biol.* **14,** 1687–1692 CrossRef Medline
39. Eyler, D. E., Burnham, K. A., Wilson, T. E., and O'Brien, P. J. (2017) Mechanisms of glycosylase induced genomic instability. *PLoS ONE* **12,** e0174041 CrossRef Medline
40. Connor, E. E., Wilson, J. J., and Wyatt, M. D. (2005) Effects of substrate specificity on initiating the base excision repair of *N*-methylpurines by variant human 3-methyladenine DNA glycosylases. *Chem. Res. Toxicol.* **18,** 87–94 CrossRef Medline
41. Zdżalik, D., Domańska, A., Prorok, P., Kosicki, K., van den Born, E., Falnes, P. Ø., Rizzo, C. J., Guengerich, F. P., and Tudek, B. (2015) Differential repair of etheno-DNA adducts by bacterial and human AlkB proteins. *DNA Repair* **30,** 1–10 CrossRef Medline
42. Calvo, J. A., Meira, L. B., Lee, C. Y., Moroski-Erkul, C. A., Abolhassani, N., Taghizadeh, K., Eichinger, L. W., Muthupalani, S., Nordstrand, L. M., Klungland, A., and Samson, L. D. (2012) DNA repair is indispensable for survival after acute inflammation. *J. Clin. Invest.* **122,** 2680–2689 CrossRef Medline
43. Baldwin, M. R., and O'Brien, P. J. (2010) Nonspecific DNA binding and coordination of the first two steps of base excision repair. *Biochemistry* **49,** 7879–7891 CrossRef Medline